This article was downloaded by:
On: *25 January 2011*
Access details: *Access Details: Free Access*
Publisher *Taylor & Francis*
Informa Ltd Registered in England and Wales Registered Number: 1072954 Registered office: Mortimer House, 37-41 Mortimer Street, London W1T 3JH, UK

## Liquid Crystals

Publication details, including instructions for authors and subscription information:
http://www.informaworld.com/smpp/title~content=t713926090

# New mesomorphic organocyclosiloxanes I. Thermal behaviour and mesophase structure of organocyclotetrasiloxanes

Elena V. Matukhina; Olga I. Shchegolikhina; Natalia N. Makarova; Yulia A. Pozdniakova; Dimitris E. Katsoulis; Yuli K. Godovsky

Online publication date: 06 August 2010

**To cite this Article** Matukhina, Elena V. , Shchegolikhina, Olga I. , Makarova, Natalia N. , Pozdniakova, Yulia A. , Katsoulis, Dimitris E. and Godovsky, Yuli K.(2001) 'New mesomorphic organocyclosiloxanes I. Thermal behaviour and mesophase structure of organocyclotetrasiloxanes', Liquid Crystals, 28: 6, 869 — 879

**To link to this Article: DOI:** 10.1080/02678290110039930

**URL:** http://dx.doi.org/10.1080/02678290110039930

PLEASE SCROLL DOWN FOR ARTICLE

Full terms and conditions of use: http://www.informaworld.com/terms-and-conditions-of-access.pdf

This article may be used for research, teaching and private study purposes. Any substantial or systematic reproduction, re-distribution, re-selling, loan or sub-licensing, systematic supply or distribution in any form to anyone is expressly forbidden.

The publisher does not give any warranty express or implied or make any representation that the contents will be complete or accurate or up to date. The accuracy of any instructions, formulae and drug doses should be independently verified with primary sources. The publisher shall not be liable for any loss, actions, claims, proceedings, demand or costs or damages whatsoever or howsoever caused arising directly or indirectly in connection with or arising out of the use of this material.

LIQUID CRYSTALS, 2001, VOL. 28, NO. 6, 869–879

# New mesomorphic organocyclosiloxanes
# I. Thermal behaviour and mesophase structure of organocyclotetrasiloxanes

ELENA V. MATUKHINA
Department of Physics, Moscow State Pedagogical University,
Malaya Pirogovskaya St. 1, Moscow 119882, Russia

OLGA I. SHCHEGOLIKHINA*, NATALIA N. MAKAROVA,
YULIA A. POZDNIAKOVA
Institute of Organoelement compounds, Russian Academy of Sciences,
Vavilova St. 28, Moscow 117813, Russia

DIMITRIS E. KATSOULIS
Dow Corning Asia Ltd., 603 Kishi, Yamakita, Kanagawa 258-0112,
Japan

and YULI K. GODOVSKY
Karpov Institute of Physical Chemistry, Vorontsovo Pole St. 10, Moscow 103064,
Russia

(*Received 14 October 2000; accepted 23 December 2000*)

*cis*-Cyclotetrasiloxanes of the formula *cis*-$[PhSi(O)(OSiMe_2R)]_4$ with $R =$ Me, $CH_2Cl$, $CH{=}CH_2$ and *cis*-$[ClC_6H_4Si(O)(OSiMe_3)]_4$ were synthesized and investigated in terms of their thermotropic phase transitions. Two ordered phases were observed for the *cis*-cyclotetrasiloxanes, one at lower temperature exhibiting the properties of a crystal and one at higher temperature exhibiting the properties of a plastically crystalline (3D) mesophase. A detailed examination of the mesophase behaviour and mesophase structure of octaphenylcyclotetrasiloxane was also carried out. It was shown that the thermal properties and structural characteristics of the mesophase are influenced by the structural characteristics of the substituent attached at the silicon atom in the tetracyclosiloxane. The new mesomorphic *cis*-cyclotetrasiloxanes are by far the largest molecules reported to date as forming plastic crystals, and the temperature region of the mesophase is much broader than in other plastic crystals. All five cyclotetrasiloxanes studied were found to be isomorphous in the 3D-mesophase and the low temperature forms of the two *cis*-cyclotetrasiloxanes: $PhSi(O)(OSiMe_2R)_4$ ($R =$ Me, $CH{=}CH_2$) were also isomorphous.

## 1. Introduction

A wealth of mesomorphic compounds exists containing different types of organic ring such as cyclohexane and bicyclo(2,2,2)octane but, apart from this very little is known about the mesomorphic behaviour of organocyclosiloxanes. As far as it can be determined information is limited to data obtained for octaphenylcyclotetrasiloxane (POCTS) [1–5]. At the same time, mesomorphic organosiloxanes with a cyclic siloxane core are of great interest as they can have important properties, such as high isotropization temperatures—similar to those of mesomorphic cyclolinear polyorganosiloxanes [6].

The aim of our studies was to examine a broad variety of cyclic organosiloxanes (CS compounds) in an attempt to identify those with mesomorphic properties, and also to understand the dependence of these properties on the chemical and geometrical structure of the molecular fragments and the molecule as a whole. Two principal ways of varying the CS structure are obvious: modification of the side groups and of the size of the siloxane

---

*Author for correspondence; e-mail: olga@ineos.ac.ru

*Liquid Crystals* ISSN 0267-8292 print/ISSN 1366-5855 online © 2001 Taylor & Francis Ltd
http://www.tandf.co.uk/journals
DOI: 10.1080/02678290110039930

ring. Note, that by changing only the substituent type, we can control two factors that govern the formation of mesomorphic structures: the molecular geometry and the distribution of the intermolecular forces. However, these factors are also influenced by the size of the siloxane ring. By varying the ring size we could also exert an influence on the molecular flexibility which is also of great importance in mesophase formation. To distinguish the influence of side groups and the CS ring size in the process of the mesophase ordering we must consider organosiloxanes in which the side groups and the ring size are changed separately and gradually.

Moreover, we need to understand the various factors which determine the fact that some members of a series of similarly shaped molecules form mesophase structures and some do not. Alongside these considerations, the question arises as to whether all the phases of previously reported CS compounds have been discovered and reliably characterized. Such an extended view will demand not only the synthesis and investigation of new CS compounds but also the detailed analysis of the well-known ones. In the first instance this applies to OPCTS, and the fact is that there is very little agreement among previous authors as to the phase behaviour and the mesophase structure of OPCTS.

Research on the mesomorphic behaviour of OPCTS was initiated by Keyes and Daniels [1] in the early 1970s and led to a number of articles concerning the thermal behaviour, the mesophase structure and properties of this compound [2–5]. The majority of researchers classified the OPCTS mesophase as plastic crystalline [1, 2, 4, 5]. The neutron scattering pattern revealed only one intense peak for the mesophase of OPCTS, suggesting a smectic A ordering [3]. X-ray diffraction (XRD) experiments on OPCTS were then carried out by Albertini *et al.* [4], who rejected a smectic A ordering, and confirmed the plastically crystalline nature of the mesophase of OPCTS. These authors interpreted the absence of additional peaks in the neutron scattering pattern as being due to changes in the sample texture over time. In our opinion there are good reasons for this interpretation, since quite similar effects connected with time-dependent changes in mesophase texture were observed in the course of our X-ray studies on two compounds from the series of oligotrimethylsiloxysiloxanes (TMSS compounds): $R\mathrm{O}[\mathrm{Si}(\mathrm{O}R)_2\mathrm{O}]_nR$, where $R$ is $\mathrm{OSi(CH_3)_3}$, namely, in hexakistrimethylsiloxydisiloxane with $n = 2$ and in octakistrimethylsiloxytrisiloxane with $n = 3$ [7]. It should be noted also that in the work of Albertini *et al.* [4], although the authors gave emphasis to the optical isotropy of the mesophase of OPCTS and came to the conclusion about its plastic crystal nature, the powder diffractogram of the mesophase given in the article did not correspond to the molecular organization in a cubic lattice. Moreover, as evidenced by detailed DSC investigations [2], on slow cooling, the transition from the mesophase to the crystalline phase in OPCTS has a two-step or even a three-step character. However, in this work, as well as in the other publications, there are no data concerning the nature of this phenomenon.

To eliminate the above contradictions and to gain a better insight into the problems related to the mesomorphic behaviour and mesophase structure of OPCTS, we decided to begin our investigations with a detailed examination of this compound. However, compounds with molecular structures similar to that of OPCTS are very relevant to studies of the mesomorphic nature of CS compounds. We therefore considered it worthwhile to extend identical studies to other non-symmetrical phenyl-substituted cyclosiloxanes. The plastically crystalline behaviour of two compounds from the TMSS series [7] suggested that phenyltriorganylsiloxy compounds could exhibit similar phases. Preliminary DSC results obtained for *cis*-$[\mathrm{PhSi(O)(OSiMe_3)}]_4$ by Feher *et al.* [8] also pointed out the possibility of mesophase formation in this CS.

As part of our general study on the thermal behaviour of organosiloxanes, we focused attention on the effect of the substituent in organocyclotetrasiloxanes (CTS compounds) and report here some results on the mesomorphic properties of OPCTS and a series of *cis*-cyclotetrasiloxanes (*c*-CTS) of formula *cis*-$[R_1\mathrm{Si(O)}R_2]_4$, which can be regarded as the triorganylsiloxy derivatives of OPCTS:

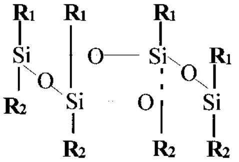

OPCTS $R_1$ = Ph, $R_2$ = Ph
**I** $R_1$ = Ph, $R_2$ = $\mathrm{OSiMe_3}$
**Ia** $R_1$ = Ph, $R_2$ = $\mathrm{OSiMe_2(CH_2Cl)}$
**Ib** $R_1$ = Ph, $R_2$ = $\mathrm{OSiMe_2(CH{=}CH_2)}$
**II** $R_1$ = $\mathrm{C_6H_4Cl}$, $R_2$ = $\mathrm{OSiMe_3}$

Unsymmetrically substituted CTS compounds were obtained by the treatment of sodium phenylsiloxanolate (SPS), *cis*-tetraphenyl- and *cis*-tetra(chlorophenyl)-(tetrahydroxy)cyclotetrasiloxanes (A1 and A2) with a corresponding triorganochlorosilane according to the scheme below.

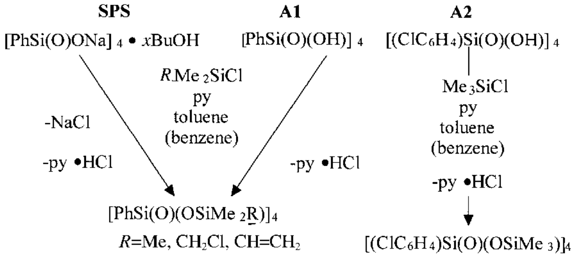

Scheme.

## 2. Experimental

### 2.1. *Materials*

Pure OPCTS was synthesized by the method described in [9]. The initial crystalline sodium phenylsiloxanolate (SPS) was prepared according to the method described in [10]. *cis*-2,4,6,8-Tetraphenyl-2,4,6,8-tetrahydroxycyclotetrasiloxane was prepared using fractional recrystallization from acetone [11 *a*] and by the reaction of SPS with a dilute solution of hydrochloric acid [11 *b*].

### 2.1.1. *Synthesis of cis-tetraphenyltetrakis-(trimethylsiloxy)cyclotetrasiloxane from SPS*

A flask was charged with $Me_3SiCl$ (9.77 g, 0.09 mol) and 3.96 g (0.05 mol) of pyridine in 60 ml benzene and 7.14 g (0.01 mol) of SPS were added at once. The resulting mixture was stirred under reflux for 1 h. After cooling to room temperature, the precipitate was filtered off and the filtrate was washed with water until a neutral $Cl^-$ ion test with $AgNO_3$ was obtained. The organic phase was then dried over anhydrous sodium sulphate. The benzene was removed *in vacuo*, and the residue was recrystallized from hot ethanol to afford 7.40 g (87.9%) of white crystals. Analysis for $\{C_6H_5Si(O)[OSi(CH_3)]_3\}_4$: found C 51.82, H 6.66, Si 26.15; calc. for $C_{36}H_{56}O_8Si_8$ C 51.38, H 6.71, Si 26.70%. $^1H$ NMR ($CCl_4$): $\delta$ 0.22 ppm (s, Me), $\delta$ 7.10–7.40 ppm (m, Ph). $^{29}Si$ NMR ($C_6D_6$): $\delta$ 10.46 ppm ($OSiMe_3$), $\delta$ – 78.97 ppm ($O_3SiPh$).

### 2.1.2. *Synthesis of cis-tetraphenyltetrakis-(trimethylsiloxy)cyclotetrasiloxane from sym-cis-[PhSi(O)OH]$_4$*

*cis*-Tetraphenyltetrakis(trimethylsiloxy)cyclotetrasiloxane was prepared according to the procedure described in [12]. $^1H$ NMR ($C_6D_6$): $\delta$ 0.38 ppm (s, Me), $\delta$ 7.10–7.64 ppm (m, Ph). $^{29}Si$ NMR ($C_6D_6$): $\delta$ 10.72 (s) ppm ($OSiMe_3$) and – 78.74 (s) ppm ($O_3SiPh$).

### 2.1.3. *Synthesis of cis-tetraphenyltetrakis[(dimethyl)-(vinyl)siloxy]cyclotetrasiloxane from SPS*

15.5 g (0.097 mol) of crystalline SPS was added to a mixture of 46.81 g (0.388 mol) of $Me_2(CH_2{=}CH)SiCl$, 23.02 g (0.291 mol) of pyridine and dry benzene (200 ml) at room temperature and vigorously stirred. The reaction mixture was then heated under reflux for 1 h. After the mixture was cooled to room temperature, it was washed with water and dried over anhydrous $Na_2SO_4$. 19.2 g (89%) of *cis*-$\{PhSi(O)[OSi(Me)_2(CH_2{=}CH)]\}_4$ were obtained after removing the solvents and drying in vacuum (1 mm Hg/80°C/1 h). Analysis for $\{C_6H_5Si(O)[OSi(CH_3)_2(CH{=}CH_2)]\}_4$: found C 53.93, H 6.47, Si 24.98; calc. for $C_{40}H_{56}O_8Si_8$ C 54.01, H 6.35, Si 25.26%. $^1H$ NMR ($CCl_3$): $\delta$ 0.27 ppm (s, Me), $\delta$ 7.20–7.49 ppm (m, Ph), $\delta$ 5.67–6.21 (m, $CH{=}CH_2$). $^{29}Si$ NMR ($CCl_4$): $\delta$ – 0.898 ppm ($OSiMe_2CH{=}CH_2$), $\delta$ – 78.815 ppm ($O_3SiPh$).

### 2.1.4. *Synthesis of cis-tetraphenyltetrakis[(dimethyl)-(vinyl)siloxy]cyclotetrasiloxane from sym-cis-[PhSi(O)OH]$_4$ (Al)*

2.07 g (0.0035 mol) of the *cis*-tetrol (Al) was added as a powder to the mixture of 3.35 g (0.0277 mol) of $Me_2(CH_2{=}CH)SiCl$, 2.19 g (0.0277 mol) of pyridine and dry toluene (30 ml) at room temperature with vigorous stirring. The reaction mass was heated under reflux for 1 h. After cooling to room temperature, the reaction mixture was washed with water and the organic layer dried over anhydrous $Na_2SO_4$. 3.07 g (98.7%) of *cis*-$\{PhSi(O)[OSi(Me)_2(CH_2{=}CH)]\}_4$ were obtained after removing the solvents and drying in vacuum (1 mm Hg/80°C/1 h). $^1H$ NMR ($CDCl_3$): $\delta$ 0.23 ppm (s, Me), $\delta$ 7.06–7.33 ppm (m, Ph), $\delta$ 5.76–6.26 (m, $CH{=}CH_2$). $^{29}Si$ NMR ($C_6D_6$): $\delta$ – 0.921 ppm ($OSiMe_2CH{=}CH_2$), $\delta$ – 78.828 ($O_3SiPh$).

### 2.1.5. *Synthesis of cis-tetraphenyltetrakis-[(chloromethyl)(dimethyl)siloxy]tetracyclosiloxane from SPS*

11.53 g (84%) of *cis*-$\{PhSi(O)[OSi(Me)_2(CH_2Cl)]\}_4$ were obtained from 8.98 g (0.056 mol) of crystalline SPS and 40.11 g (0.28 mol) of chloromethyldimethylchlorosilane in 170 ml of toluene in the presence of pyridine (17.71 g, 0.224 mol). Analysis for $\{C_6H_5Si(O)[OSi(CH_3)_2(CH_2Cl)]\}_4$: found C 45.11, H 5.80, Si 22.33, Cl 14.22; calc. for $C_{36}H_{52}Cl_1O_8Si_8$ C 44.15, H 5.35, Si 22.95, Cl 14.48%. $^1H$ NMR ($C_6D_6$): $\delta$ 0.36 ppm (s, Me), $\delta$ 2.78 ppm (s, $CH_2Cl$), $\delta$ 6.91–7.55 ppm (m, Ph). $^{29}Si$ NMR ($C_6D_6$): $\delta$ 5.940 ppm ($OMe_2CH_2Cl$), $\delta$ – 78.13 ($O_3SiPh$).

### 2.1.6. *Synthesis of cis-tetraphenyltetrakis-[(chloromethyl)(dimethyl)siloxy]tetracyclosiloxane from sym-cis-[PhSi(O)OH]$_4$ (Al)*

3.68 g (86.38%) of the required product were obtained from 2.6 g (0.0044 mol) of *cis*-tetrol (Al) and 7.48 g (0.052 mol) of $Me_2(CH_2Cl)SiCl$ in 50 ml of benzene in the presence of pyridine (4.11 g, 0.052 mol). $^1H$ NMR ($C_6D_6$): $\delta$ 0.35 ppm (s, Me), $\delta$ 2.78 ppm (s, $CH_2Cl$), $\delta$ 6.91–7.53 ppm (m, Ph). $^{29}Si$ NMR ($C_6D_6$): $\delta$ 5.89 ppm ($OMe_2CH_2Cl$), $\delta$ – 78.14 ($O_3SiPh$).

### 2.1.7. *Synthesis of cis-tetra(chlorophenyl)tetrakis-(trimethylsiloxy)cyclotetrasiloxane*

*cis*-Tetra[(hydroxy)(chlorophenyl)]cyclotetrasiloxane was first obtained in a yield of 9.6% by hydrolysis of chlorophenyltrichlorosilane. The low yield reflects the fact that the hydrolysis of monomers of the type $R SiCl_3$ is a multistep, complicated process leading to various products including crosslinked 3D-networks, ladder-like oligomers, polyhedral silsesquioxanes, etc. A solution of 213 g (0.866 mol) of chlorophenyltrichlorosilane in either (200 ml) was added dropwise to a mixture of water and ether (300 ml/300 ml) with vigorous stirring (temperature, 3–5°C, addition time 2 h). The ethereal phase as separated off, washed with water until neutral, and dried over anhydrous $Na_2SO_4$; the ether was then evaporated. A white precipitate was formed after the addition of 200 ml of toluene to the residue. Washing several times with toluene and pentane yielded 14.40 g (9.6%) of white crystals, m.p. 210–214°C.

A benzene/ether (3 ml/8 ml) solution of 0.69 g (0.001 mol) of the above product *cis*-$[ClC_6H_4Si(O)OH]_4$ and 0.318 g (0.004 mol) of pyridine was added to 2 ml of a benzene solution containing 0.868 g (0.008 mol) of $Me_3SiCl$, and the mixture stirred for 8 h at room temperature. Then 8 ml of benzene were added and the reaction mixture was heated to 60°C and stirred for 6 h. The benzene solution obtained after filtration from the precipitate of pyridine hydrochloride was washed several times with water. The solvent was removed to give 0.47 g (44.9%) of a white solid, m.p. 52–58°C. The crude product was recrystallized from benzene/ethanol, followed by sublimation under vacuum (0.01 mm Hg, 250°C) yielding 0.30 g (28.7%) of white crystals, m.p. 56.5–57.5°C. Analysis for $\{ClC_6H_4Si(O)[OSi(CH_3)_3]\}_4$: found C 44.59, H 5.48, Si 22.75, Cl 14.53; calc. for $C_{36}H_{52}Cl_1O_8Si_8$ C 44.15, H 5.35, Si 22.95, Cl 14.48%. $^1$H NMR ($C_6D_6$ + $CCl_4$): $\delta$ 0.033 ppm (s, 9H, Me), $\delta$ 7.05–7.29 ppm (m, $C_6H_4Cl$). $^{29}$Si NMR ($C_6D_6$ + $CCl_4$): $\delta$ 11.92 ppm ($OSiMe_3$), $\delta$ – 80.36 ($O_3SiC_6H_4Cl$).

### 2.2. *Measurements*

The $^1$H and $^{29}$Si NMR spectra were obtained, respectively, on a Bruker DRX-500 spectrometer operating at 500 MHz and at 99.325 MHz at 20°C in $CD_3Cl$ and in $C_6D_6$. Chemical shifts are reported relative to TMS as the internal reference standard.

The thermal characteristics of glass and phase transitions were obtained from differential scanning calorimetry (DSC) scans, which were recorded on a Perkin-Elmer DSC-7 at a heating rate of 10°C min$^{-1}$ from ambient temperature up to the sublimation temperature. The sublimation temperatures were established by thermogravimetric analysis (TGA) using a 'Derivatograph-K' (MOM Production, Hungary). TGA measurements were carried out in air. The TGA sample size was 20–30 mg and the heating rate was 5°C min$^{-1}$. The temperature at which a weight loss of 2% was detected was considered as the onset of the sublimation process.

X-ray characterization was performed with filtered CuK$_\alpha$ radiation using a DRON-3M X-ray diffractometer with an asymmetric focusing monochromator (a bent quartz crystal), equipped with a heating and a cooling camera wherein the temperature was automatically regulated. X-ray diffraction (XRD) patterns were obtained over a wide temperature range. Phase diagrams were deduced from these diffraction patterns. During each experiment the temperature of the sample was controlled to better than ± 1°.

The assignments of the transition temperatures were confirmed by polarizing optical microscopy (POM). Optical birefringence studies were carried out using a Mettler FP2 temperature-programmable hot stage and a microscope with crossed polarizers.

## 3. Phase transition behaviour

### 3.1. *Octaphenylcyclotetrasiloxane (OPCTS)*

According to the DSC curves presented in figure 1, OPCTS exhibits three reversible transitions. Comparison of the DSC and X-ray data (figures 1 and 2) indicates that heating above the first transition results in a change in crystalline structure, whereas at the second transition the crystals melt and OPCTS remains in a mesomorphic state until the third transition (isotropization temperature). The temperatures of the transitions are summarized in the table, and the X-ray patterns of the crystalline modifications are in agreement with data reported earlier [2, 12].

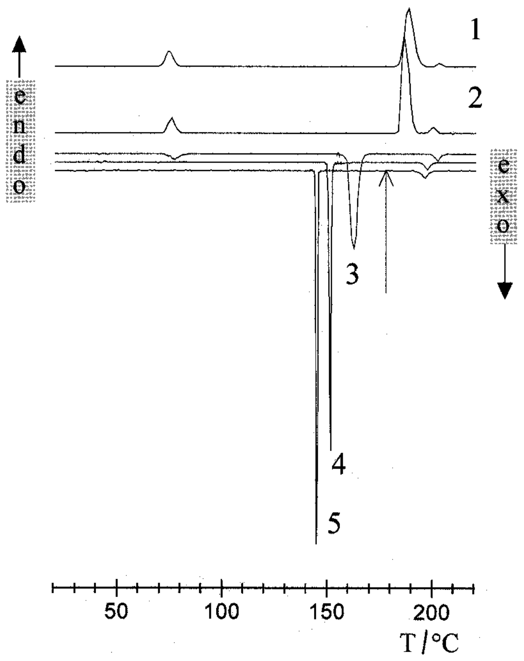

Figure 1. DSC curves for OPCTS obtained on heating (curves 1, 2) and cooling (curves 3, 4, 5) at various scan speeds: curve 1, 10 K min$^{-1}$; curve 2, 5 K min$^{-1}$; curve 3, – 10 K min$^{-1}$; curve 4, – 5 K min$^{-1}$; curve 5, – 0.5 K min$^{-1}$. Arrow marks the temperature corresponding to the appearance of birefringence on cooling.

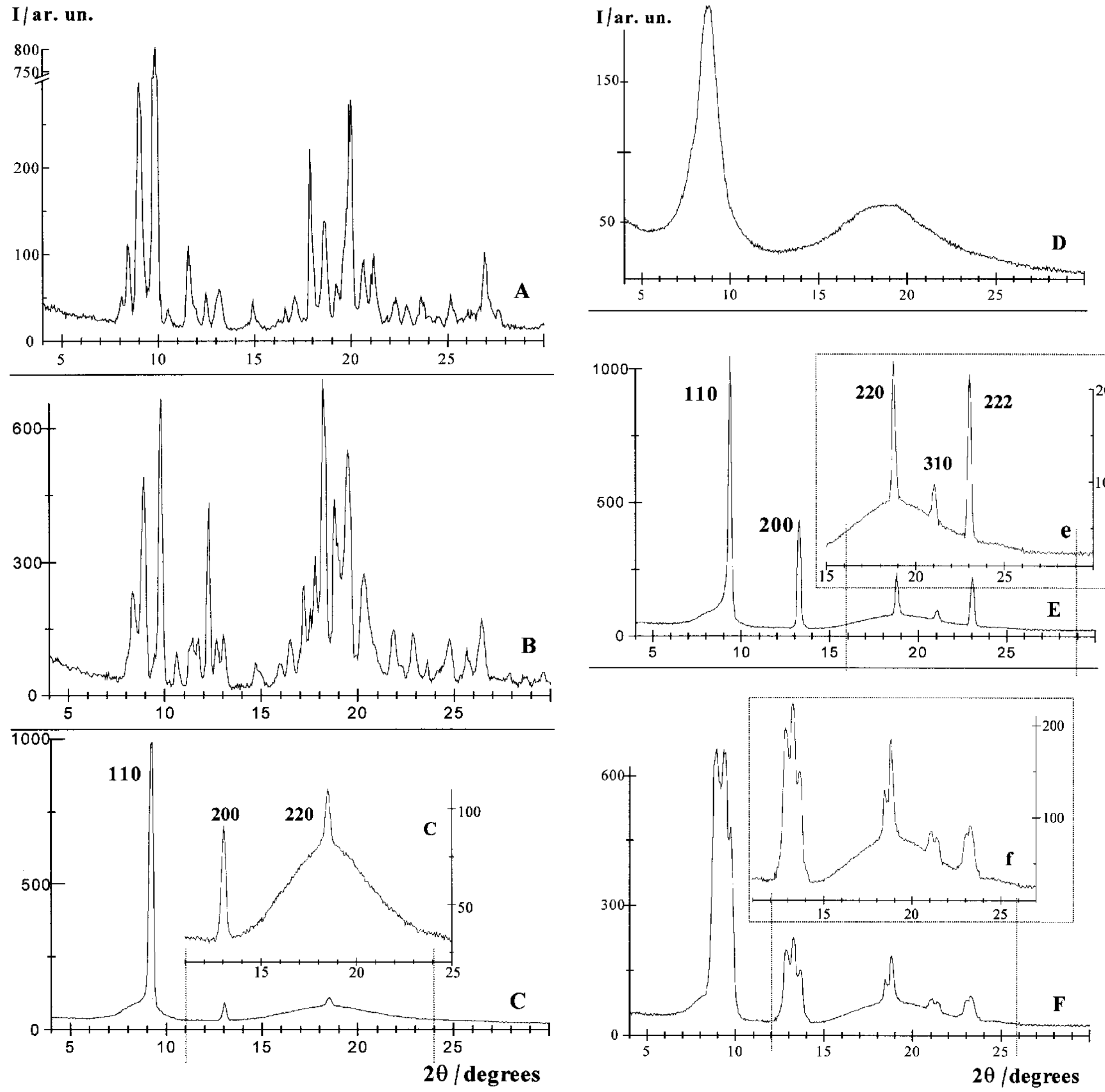

Figure 2. X-ray patterns of OPCTS obtained on heating (curves A, B, C, D) and on slow cooling from 198°C (curves E, F). Curve A 20°C; curve B 100°C; curve C 198°C; curve D 210°C. Curve E 178°C; curve F 168°C.

The XRD patterns of OPCTS obtained on heating (figure 2, curve C) show features characteristic of diffractograms of a plastic crystalline mesophase. Indeed, the diffraction pattern of the mesophase presents only three Bragg peaks, the intensities of the reflections decreasing vary rapidly with increasing Bragg angle $\theta$. The angular positions of the mesophase reflections appear to be very sensitive to temperature change. Moreover, a strong diffuse scattering in the form of two broad halos is observed underneath the Bragg peaks. The values of $\sin^2 \theta$ for the neighbouring peaks are in the ratio 1:2:4, and this suggests the existence of cubic symmetry for the mesophase. This is confirmed by optical microscopic examination: the mesophase in the temperature region 190–203°C is optically isotropic. The transition from the mesomorphic to the isotropic state occurs at 205°C: after isotropization only two broad maxima are observed (figure 2, curve D).

According to the DSC and X-ray data, the transition from crystal to mesophase displays considerable hysteresis and on cooling it occurs at temperatures that are 40–50° lower than the temperature observed on heating. The diffraction pattern of the supercooled mesophase at 178°C is sharper due to a reduction in molecular motion: five Bragg peaks are observed (figure 2, curve E). The values of $\sin^2 \theta$ for the neighbouring peaks are in the ratio 1:2:4:5:6, additionally confirming the cubic symmetry of the OPCTS mesophase.

On slow cooling, the appearance of birefringence was at 174°C, at a temperature substantially higher than the crystallization temperature detected by DSC. Indeed, as figure 1 shows, $T_{cr} = 145°C$, when cooling rate was

Table. Thermal characteristics of the organocyclotetrasiloxanes. **I** $R_1$ = Ph, $R_2$ = OSiMe$_3$; **Ia** $R_1$ = Ph, $R_2$ = OSiMe$_2$(CH$_2$Cl); **Ib** $R_1$ = Ph, $R_2$ = OSiMe$_2$(CH=CH$_2$); **II** $R_1$ = C$_6$H$_4$Cl, $R_2$ = OSiMe$_3$.

| | DSC[a] | | | | | | | TGA |
|---|---|---|---|---|---|---|---|---|
| | Cold crystallization | | | Crystal ↓↑ Mesophase | | Mesophase ↓↑ Isotropic melt | | Sublimation[b] |
| Compound | $T_g$/°C | $\Delta T_{ccr}$/°C | $\Delta H$/J g$^{-1}$ | $T_m$/°C | $\Delta H$/J g$^{-1}$ | $T_i$/°C | $\Delta H$/J g$^{-1}$ | $T_{sb}$/°C |
| (A) | — | — | — | 186 | 56.5 | 200 | 1.6 | 330 |
| OPCTS (B) | — | — | — | 149 | 53.2 | 199 | 2.1 | |
| (C) | — | — | — | 183 | 57.9 | 202 | 2.5 | |
| (A) | — | — | — | 78 | 25.9 | 262 | 2.1 | 242 |
| **I** (B) | — | — | — | 29 | 21.8 | 258 | 2.2 | |
| (C) | — | — | — | 64 | 24.9 | 263 | 1.9 | |
| (A) | — | — | — | 45 | 18.7 | c | | 260 |
| **Ia** (B) | $-69$ | — | — | — | — | | | |
| (C) | $-64$ | $-40 \rightarrow -11$ | 15.8 | 43 | 16.7 | | | |
| (A) | $-78$ | — | — | 31 | 16.6 | 273 | 4.2 | 255 |
| **Ib** (B) | $-82$ | — | — | — | — | 264 | 3.6 | |
| (C) | $-77$ | $-63 \rightarrow -46$ | 13.8 | 28 | 15.4 | 266 | 3.9 | |
| (A) | $-69$ | — | — | 59 | 59.0 | c | | 235 |
| **II** (B) | $-60$ | — | — | — | — | | | |
| (C) | $-67$ | $-28 \rightarrow 12$ | 46.5 | 55 | 51.6 | | | |

[a] (A) First heating; (B) cooling; (C) second heating.

[b] Temperature at which a weight loss of 2% was detected.

[c] The specimen sublimes directly without isotropization.

0.5 K min$^{-1}$. Note that on cooling, DSC revealed no transition in the temperature range 145–190°C. This evidence led us to the conclusion that the cooling process was accompanied by a transformation from a high temperature enantiotropic (HT-) mesophase to a low temperature monotropic (LT-) phase. This conclusion is supported by the corresponding X-ray data.

The changes in the scattering pattern observed on cooling show that crystallization was preceded by at least one polymesomorphic transition accompanied by a lowering of the lattice symmetry of the mesophase. The pattern observed at 160°C revealed only a splitting of the peaks of the HT-mesophase; the characteristic features of a plastically crystalline mesophase were simultaneously preserved. So the monotropic non-cubic (birefringent) mesomorphic modification must also be attributed to a plastically crystalline phase. Note that rare examples of non-cubic plastic crystals have been described in the literature [13]. The features of the X-ray pattern after the transition to the monotropic mesophase, as well as the absence of any thermal effects on the DSC curves in the temperature range 145–190°C, suggest that the LT-mesophase appears as a consequence of deformation along one of the symmetry axes of the cubic crystals. In other words the transition to the monotropic mesophase is similar to solid–solid transitions that are usually considered as second order phase transitions.

In the case of plastic crystals the lowering of the lattice symmetry should be connected with a restriction of the molecular rotational mobility. In the case of OPCTS, this effect most probably occurs as a consequence of the constrained mobility of the Ph-groups, leading to the emergence of anisotropy of the molecular interactions. It is known [5], that high mobility of the Ph-groups is characteristic of OPCTS molecules in the HT-mesophase. Thus, the main effect of the Ph-groups seems to be a steric hindering of the molecule on cooling. As soon as the mobility of Ph-groups is sufficiently low, below 170°C, a non-cubic monotropic mesophase arises.

### 3.2. *Asymmetric cis-cyclotetrasiloxanes*

Figure 3 shows the DSC scans of compounds **I**, **Ia, Ib** and **II** in consecutive heating and cooling cycles. The thermal characteristics of the *c*-CTSs are given in the table.

Let us first concentrate attention on the data obtained for **I**, i.e. for the *c*-CTS without any functional groups. The specific heat curves for **I** reveal two completely reversible transitions. As can be seen from the table, the temperature of the second transition is higher than the temperature of commencement of sublimation.

Diffraction patterns recorded for **I** at temperatures below 80°C are typical for a crystalline phase (figure 4, curve A). As the temperature is raised to above 80°C

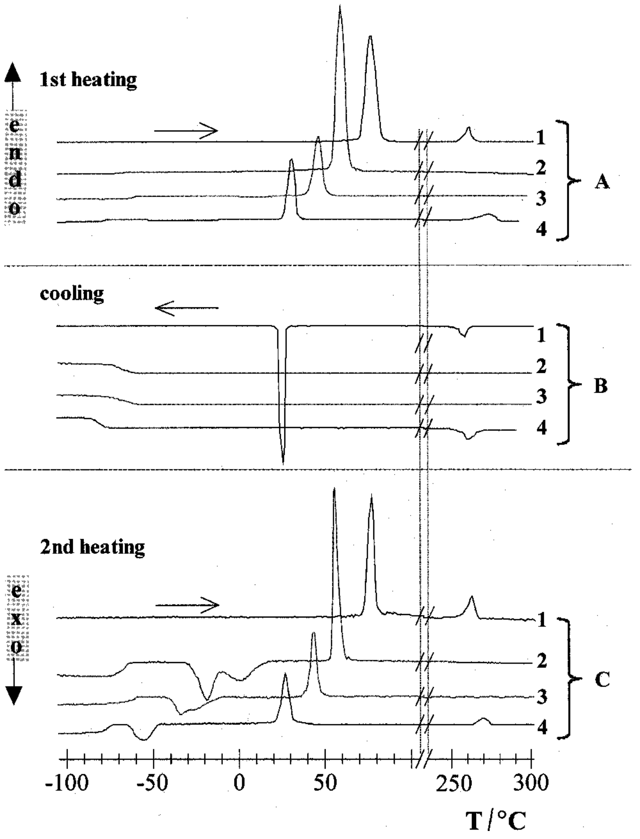

Figure 3. DSC curves of compounds **I** (1), **II** (2), **Ia** (3) and **Ib** (4): first heating (set A); cooling (set B); second heating (set C). Note the temperature axis break eliminating the region with no thermal effects. Scan speed 10 K min$^{-1}$.

there is a sharp change in the diffraction pattern which corresponds to the crystal → mesophase transition. At this transition the Bragg peaks of the crystalline phase disappear; in the mesophase only two sharp Bragg peaks (Bragg max. 1/2 = 0.25 degrees) and one amorphous halo (Bragg max. 1/2 = 5 degrees) are detected, the second Bragg peak of quite low relative intensity (figure 4, curve B). Further heating in the mesophase causes the intensity of the second peak to decrease. The XRD pattern of the mesophase of **I** (figure 4, curve B) is quite similar to the XRD pattern of the mesophase of OPCTS, showing all the above-named features inherent in diffractograms of cubic plastic crystals [13].

The temperature of the crystal–mesophase transition depends on the direction in which the transition is approached; on cooling it occurs at lower temperatures. The diffraction patterns of the supercooled mesophase of **I** exhibits five peaks (figure 4, curve C). The ratio 1 : 2 : 3 : 5 : 8 between the values of $\sin^2 \theta$ for neighbouring peaks confirms the cubic symmetry of the mesophase. This ratio appears to be constant over the whole temperature range of existence of the mesophase (25–270°C), while the intensities of the peaks decrease as the isotropization point is approached and above 80°C only two peaks can be detected. The transition from the mesomorphic to the isotropic state occurs over a wide temperature range from 250°C up to 270°C (figure 4, curve E) and is accompanied by an intense sublimation process.

Considering the DSC data obtained for the *c*-CTSs that contain functional groups (figure 3) one can see, that the DSC traces (2, 3 and 4) obtained on first heating run reveal two transitions for **Ib** and one transition each for **Ia** and **II**. The cooling curve (4) of **Ib** shows only one exothermic peak in the high temperature region. The cooling DSC cycles for **Ia** and **II** show no enthalpy change for the transition back to the solid: there is a slight rise in the base line suggesting that the materials set into glassy state. On second heating of **Ia**, **Ib** and **II** exothermic peaks were observed just above the glass transition temperatures, indicating that in each case an ordered structure was formed. On further heating the melting peaks were observed.

As can be seen from figures 5–7, the diffraction patterns obtained on heating and cooling **Ia**, **Ib** and **II** revealed two ordered phases with that at lower temperatures exhibiting the properties of a typical crystal and that at higher temperatures exhibiting features characteristic of the mesophase of **I**. The mesophase of **Ia**, **Ib** and **II** is analogous in other ways to that of **I**. For instance, it can be supercooled. Note that the transition crystal → mesophase for **Ia**, **Ib** and **II** showed highly rate-dependent supercooling. With the cooling rate of 1 K min$^{-1}$ used in the X-ray system, this transition supercools as much as 30°C. However, even for the supercooled mesophase of **Ia**, **Ib** and **II**, it is impossible to detect more than two reflections: the first is very strong, the second is very weak. The values of $\sin^2 \theta$ for these peaks are in the ratio 1 : 2, and based on that we again propose a cubic symmetry for the mesophases of **Ia**, **Ib** and **II**.

## 4. Mesomorphic properties

### 4.1. *The type of ordering in the mesophase*

To sum up the information about the mesophase behaviour of the CTS materials studied, we can conclude that all these tetramers exhibit numerous analogies with plastic crystals [13, 14]: optical isotropy, cubic unit cells, low isotropization enthalpies, plasticity, etc. The estimated value of $\Delta H$ for the mesophase to isotropic melt is of the same order as that for compounds exhibiting plastic crystalline phases [14]. It should be noted that the mesophase of the CTS materials was not as transparent as the isotropic phase and it was possible to observe the transition from the isotropic liquid to the mesophase in ordinary light for OPCTS, **I** and **Ib**.

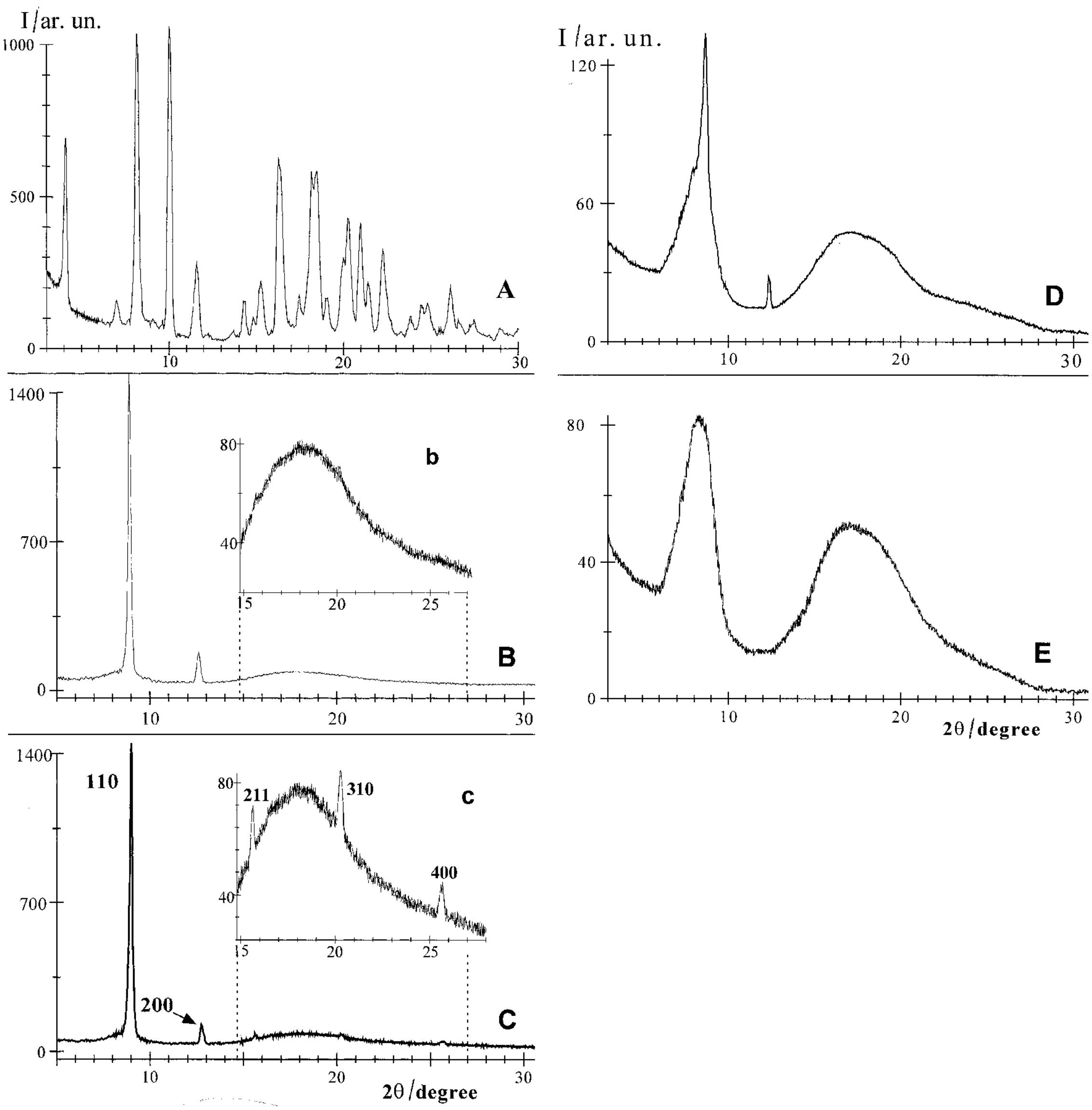

Figure 4. X-ray patterns of **I** at 20°C (A), 83°C (B, b), 30°C after cooling from 83°C (C, c), 250°C (D), and 265°C (E). The decrease of the integral intensity observed at temperatures above 240°C (curves D and E) is connected with intense sublimation, see the table.

The small number of observed Bragg peaks prevents us from estimating the space group of the cubic mesophases. For this reason, we have restricted attention to the determination of the type of a cubic lattice. Reflections were indexed on the assumption of distinct types of cubic unit cell. The packing coefficient *k* [15] served as a criterion for the correction of the chosen unit cell. We have established that the packing coefficients *k* calculated on the assumption of a body-centred molecular arrangement are the only ones giving good agreement with the real values of *k* for the mesomorphic state of all the CTS compounds.

For instance, the peaks observed in the OPCTS mesophase can be indexed as the 1 1 0, 2 0 0, 2 2 0, 3 1 0 and 2 2 2 reflections of a three-dimensional body-centred cubic (bcc) lattice (figure 2, curves C, E). The bcc unit cell contains two molecules; $a = 13.43 \pm 0.05$ Å, $k = 0.62$, $\rho = 1087\ \mathrm{kg\ m^{-3}}$ at $T = 192$°C. Unfortunately, the small number of reflections did not allow us to derive the lattice structure characteristics of the non-cubic LT-mesophase. The X-ray method of homology usually used for analogous transitions in ordinary crystals [16] did not yield good results.

The high temperature ordered phases (3D-mesophases) of all the CTS compounds under study were found to be isomorphous, unaffected by the special features of the molecules. Moreover, the low temperature crystalline forms of the two *cis*-cyclotetrasiloxanes, **I** and **Ia**, appear

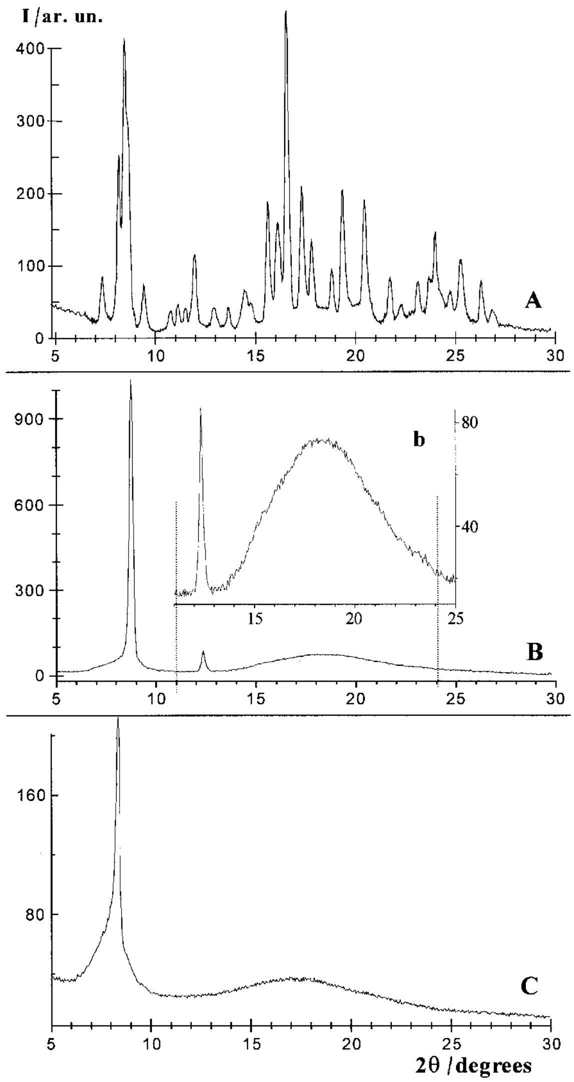

Figure 5. X-ray patterns of **Ia** at 20°C (A), 48°C (B, b) and 265°C (C). The decrease in intensity observed at 265°C (curve C) is connected with the sublimation at this temperature, see the table.

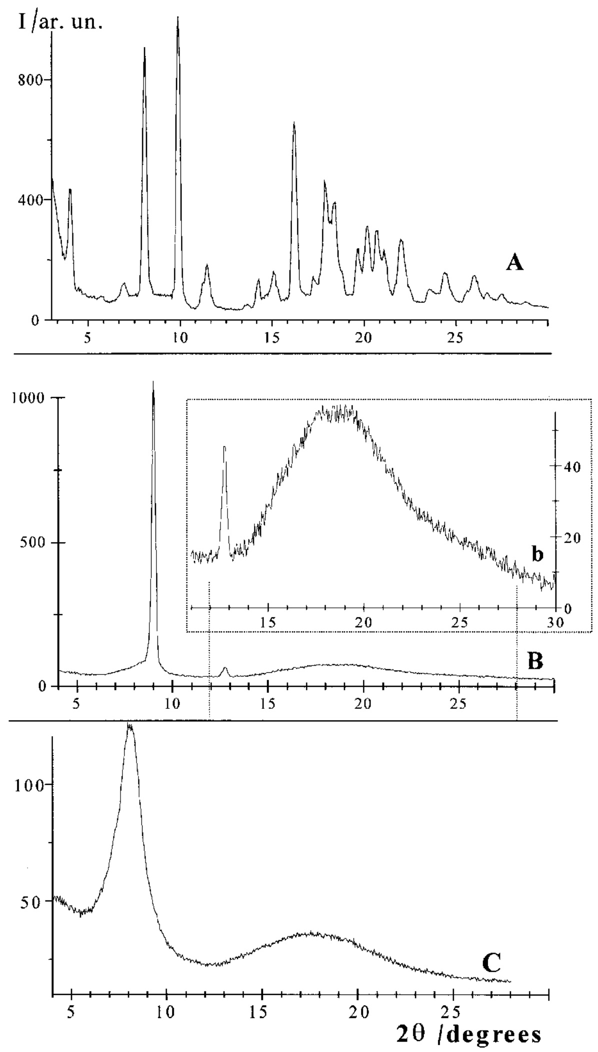

Figure 6. X-ray patterns of **Ib** at − 10°C (A), 28°C (B, b) and 270°C (C). The decrease in intensity observed at 270°C (curve C) is connected with the intense sublimation at this temperature, see the table.

to be isomorphous too, Isomorphism is supported by the formation of complete solid solutions as demonstrated for combinations of these CTS compounds. Work on the phase diagrams for several selected pairs is now in progress and will be the subject of a forthcoming paper.

### 4.2. *The effect of the side groups on the thermal and structural characteristics of the mesophase*

The data obtained from the study of all the CTS compounds suggest that the type of side group changes the structural and thermal properties of the CTS mesophase.

The structural organization of the mesomorphic state for all the CTSs is alike: they are plastic crystals, with the molecular centres of gravity located in the bcc lattice. Linear dependences of the bcc lattice parameter $a$ on temperature for all tetramers were found (figure 8) and tentative calculations of the $k$ values were made (figure 9).

The low symmetry of the static CTS molecules does not correspond with a bcc lattice, and the rotation of the molecules inherent to the plastically crystalline state is intrinsic to the CTS mesophase. The diameters of the spheres of molecular rotation established for the tetramers by using molecular models are considerably larger than the distances between the molecular centres in the bcc unit cells, $r = 0.866a$ Å. Hence, the rotation of the molecules in the mesophase must be subject to steric hindrance.

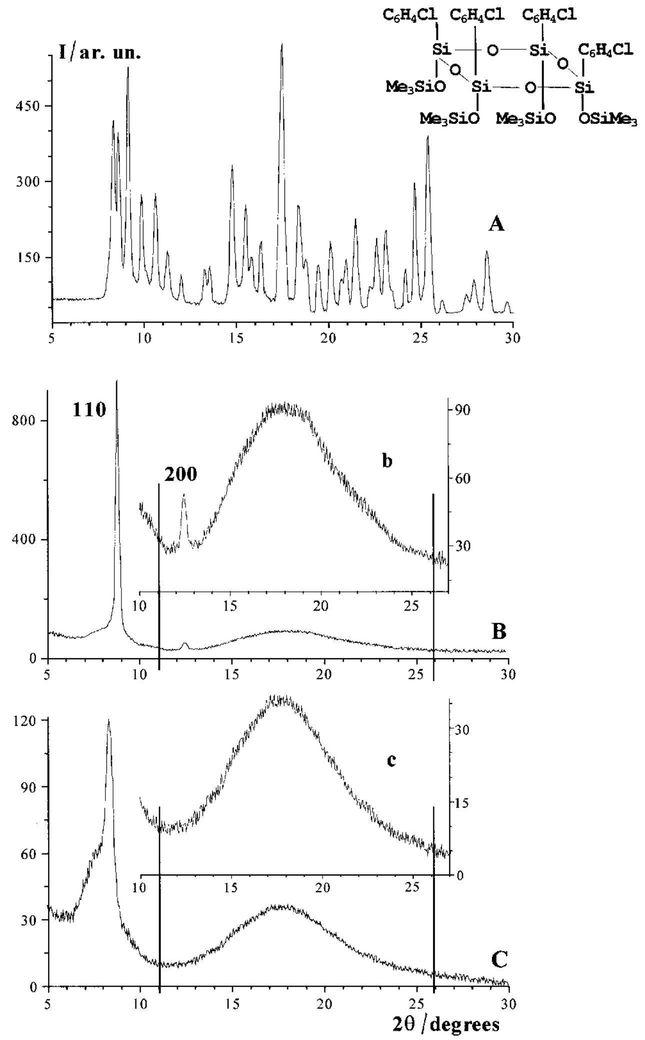

Figure 7. X-ray patterns of **II** at 20°C (A), 65°C (B, b) and 252°C (C, c). The sharp decrease in intensity observed at 252°C (curves C, c) is connected with the intense sublimation at this temperature, see the table.

As one can see from figure 8, the sizes of the molecules of **I** ($\Sigma\Delta V_i = 804.5\,\text{Å}^3$), **Ia** ($\Sigma\Delta V_i = 853.9\,\text{Å}^3$), **Ib** ($\Sigma\Delta V_i = 863.9\,\text{Å}^3$) and **II** ($\Sigma\Delta V_i = 860.5\,\text{Å}^3$) are larger than for OPCTS ($\Sigma\Delta V_i = 745.2\,\text{Å}^3$) and this results quite naturally in the increase of the bcc lattice parameter *a* and hence in the increasing distance between nearest neighbouring molecules. ($\Sigma\Delta V_i$ is the sum of the van der Waals volumes calculated from the values for the atoms forming a molecule [17].) Of the tetramers described, the molecules **Ib**, which exhibit the largest bcc unit cell, are characterized by the largest value of $\Sigma\Delta \mathbf{V}_\mathbf{i}$.

The structural identity of the mesomorphic state for all tetramers seems to be the consequence of the geometrical similarity of the molecules. Really, for the tetramers under study, the longitudinal dimensions and the van der Waals volumes of the side groups differ rather slightly. Thus, the $\Sigma\Delta V_i$ values are 79.7, 91.4, 103.7, 106.5, and 93.70 Å$^3$ for $-C_6H_5$, $-OSi(CH_3)_3$, $-OSi(CH_3)_2(CH{=}CH_2)$, $-OSi(CH_3)_2(CH_2Cl)$, and $-C_6H_4Cl$, respectively. Therefore, changing the tetramers' chemical constitution by

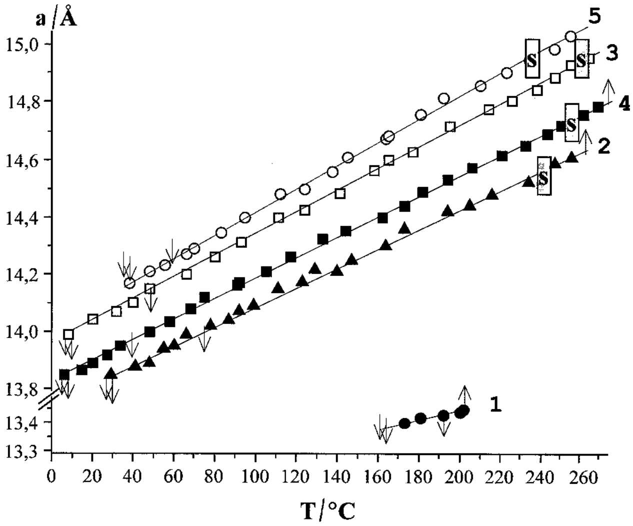

Figure 8. Temperature dependences of the parameter *a* of the bcc unit cell of OPCTS (curve 1), **I** (curve 2), **Ia** (curve 3), **Ib** (curve 4) and **II** (curve 5). Note the *a*-axis break eliminating the region without any data. The arrows define the limits of the temperature region of the mesomorphic state established by X-ray measurements: ↓—the temperature of crystal ⇒ mesophase transition (heating run); ↓↓—the temperature of mesophase ⇒ crystal transition (cooling run); ↑—the isotropisation temperature. The tetramers **Ia** (curve 3) and **II** (curve 5) sublime without isotropisation. The sublimation onset is marked by the symbol $\boxed{\text{S}}$.

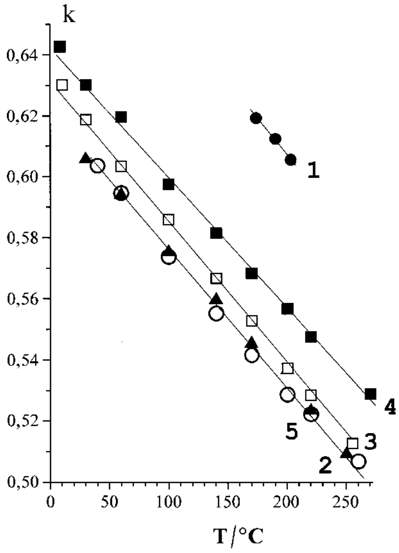

Figure 9. Temperature dependences of the packing coefficient *k* of the bcc unit cell of OPCTS (curve 1), **I** (curve 2), **Ia** (curve 3), **Ib** (curve 4) and **II** (curve 5).

using only these five types of side groups does not lead to any marked difference in the geometry of the molecules as a whole: the molecules maintain the somewhat oblate spheroidal form with no very pronounced asymmetry that is inherent to OPCTS [5]. One more factor promoting the plastically crystalline mesophase is the compact structure of the side groups, allowing them to fill the space on all sides of the tetrasiloxane cycle.

The most remarkable difference between the mesomorphic behaviour of OPCTS and the unsymmetrically substituted tetramers **I**, **Ia**, **Ib** and **II** is that the presence of the triorganylsiloxy groups results in a considerable broadening of the temperature range of the mesophase, basically owing to the shift of the crystal–mesophase transition to substantially lower temperatures. This effect can be explained by taking into account the fact that the transition from the crystal phase to the plastically crystalline mesophase is accompanied by an appreciable increase in the mobility of the side groups, creating sufficient free volume for the molecule to reorient within its cage. In the case of OPCTS this was shown by NMR studies [5]. Since for the tetramers under study, a high mobility of the triorganylsiloxy groups is possible at relatively low temperatures as compared with that for the phenyl groups, the tetramers containing triorganylsiloxy groups are characterized by markedly lower temperatures of transition to the mesophase. The additional lowering of the thermal stability of the crystalline phase after incorporating chlorine into the Ph-group seems to be a consequence of a reduction in the molecular interactions.

The presence of triorganylsiloxy groups as side substituents in the tetramers leads also to a slight rise in the thermal stability of the mesophase. This is likely to be related to the closer molecular packing in the mesophase inherent to **I**, **Ia**, **Ib** and **II** in comparison with OPCTS.

In undergoing considerable supercooling of the mesophase, the behaviour of **I**, **Ia**, **Ib** and **II** is similar to that for OPCTS. However, in contrast to OPCTS, the tetramers **I**, **Ia**, **Ib** and **II** do not undergo a polymesomorphic transition. This seems therefore to be connected with the presence of the triorganylsiloxy groups which reduce the influence of Ph-groups on the molecular free rotation.

To conclude the discussion, note that the analysis of the data obtained for the tetramers enables us to differentiate two factors related only to the exteriors of the molecules that have quite distinct influences on their mesomorphic properties, that is the *geometry* and the *elemental composition* of the side groups. The other interesting aspect is of course to understand the effect of the geometry of a CS molecule itself on the mesophase behaviour by changing only the cycle size. This can be accomplished by a comparative analysis of the data obtained for the tetramers and the hexamers, and will be considered in a forthcoming article.

Financial support of this work by the Dow Corning Corporation is gratefully acknowledged. The work involving X-ray measurements was carried out within the program 'Universities of Russia'.

## References

[1] Keyes, P. H., and Daniels, W. B., 1975, *J. chem. Phys.*, **62,** 2000.

[2] Smith, G. W., 1979, *Phase Transitions*, **1,** 107.

[3] Volino, F., and Dianoux, A. J., 1978, *Ann. Phys.*, **3,** 151.

[4] Albertini, G., Dubini, B., Melone, S., Rustichelli, F., and Torquati, G., 1980, in *Liquid Crystals of One- and Two-dimensional Order*, Springer Series in Chemical Physics, 11 (Berlin, New York), pp. 53–56.

[5] Bee, M., and Dianoux, A. J., 1984, *Mol. Phys.*, **51,** 221.

[6] Godovsky, Yu. K., Makarova, N. N., and Matukhina, E. V., 1998, *Polym. Prepr.*, **39,** 485.

[7] Matukhina, E. V., Kuzmin, N. N., and Antipov, E. M., 1989, *Dokl. Akad. Nauk SSSR*, **304,** 904.

[8] Feher, F. J., Schwab, J. J., Soulivong, D., and Ziller, L. W., 1997, *Main Group Chem.*, **2,** 123.

[9] Burkhard, C., 1945, *J. Am. chem. Soc.*, **67,** 2173.

[10] Shchegolikhina, O., Pozdniakova, Yu., Antipin, M., Katsoulis, D., Auner, N., and Herrschaft, B., 2000, *Organometallics*, **19,** 1077.

[11] (*a*) Brown, J. F., 1965, *J. Amer. chem. Soc.*, **87,** 4317; (*b*) Shchegolikhina, O. I., Molodtsova, Yu. A., Korkin, S. D., Bukalov, S. S., Leites, L. A., Lissenko, K. A., Auner, N., and Katsoulis, D. E. (to be published).

[12] Hossain, M. A., Hursthouse, M. B., and Malik, M. A., 1979, *Acta crystallogr.*, **35,** 522.

[13] Sherwood, N. (editor), 1979, *The Plastically Crystalline State. (Orientationally-disordered Crystals)* (Wiley New York, London).

[14] Winsor, P. A., 1974, in *Liquid Crystals and Plastic Crystals*, edited by G. W. Gray and P. A. Winsor (Chichester: Wiley), pp. 48–59.

[15] Kitaigorodsky, A. I., 1973, *Molecular Crystals and Molecules*, No. 29 in the series 'Physical Chemistry', edited by Ernest M. Loebl (New York, London: Academic Press).

[16] Mirkin, L. I., 1961, *Reference Book on X-ray Analysis of Polycrystals* (Moscow: Fiz.-mat. lit.) (in Russian).

[17] Meladse, S. M., Mukbaniani, O. V., Makarova, N. N., and Khananashvili, L. M., 1980, *Zh. obshch. Khim.*, **50,** 2493.